The Journal of Chemical Physics

A new, definitive analysis of a very old spectrum: The highly perturbed $A^2\Pi_u$–$X^2\Pi_g$ band system of the chlorine cation (Cl_2^+)

Cite as: J. Chem. Phys. **137**, 194317 (2012); https://doi.org/10.1063/1.4765334
Submitted: 17 September 2012 . Accepted: 18 October 2012 . Published Online: 21 November 2012

Mohammed A. Gharaibeh, Dennis J. Clouthier, Apostolos Kalemos, Hélène Lefebvre-Brion, and Robert W. Field

AIP Publishing

A new, definitive analysis of a very old spectrum: The highly perturbed $A^2\Pi_u$–$X^2\Pi_g$ band system of the chlorine cation (Cl_2^+)

Mohammed A. Gharaibeh,[1] Dennis J. Clouthier,[1,a)] Apostolos Kalemos,[2] Hélène Lefebvre-Brion,[3] and Robert W. Field[4]
[1]*Department of Chemistry, University of Kentucky, Lexington, Kentucky 40506-0055, USA*
[2]*Department of Chemistry, Laboratory of Physical Chemistry, National and Kapodistrian University of Athens, Athens 157 71, Greece*
[3]*Institut des Sciences Moléculaires d'Orsay, Bât. 210, Université de Paris Sud, 91405 Orsay Cedex, France*
[4]*Department of Chemistry, Room 6-219, Massachusetts Institute of Technology, Cambridge, Massachusetts 02139, USA*

(Received 17 September 2012; accepted 18 October 2012; published online 21 November 2012)

The laser-induced fluorescence spectrum of jet-cooled chlorine cation has been recorded in the 500−312 nm region with high sensitivity and rigorous vibrational and spin-orbit cooling. More than 80 bands of the highly vibrationally perturbed $A\,^2\Pi_u$–$X\,^2\Pi_g$ electronic transition have been detected and shown to originate from the $\Omega = 3/2$ spin-orbit component of $v = 0$ of the ground state. The spectrum extends some 3700 cm^{-1} to the red of any previously published report and the 0–0 band has been identified for the first time. The bands have regular rotational structure but exhibit irregular vibrational intervals and isotope splittings. Our *ab initio* studies show that the perturbations are due to a $\Delta\Omega = 0$ spin-orbit interaction between the $A^2\Pi_{3/2u}$ and $B^2\Delta_{3/2u}$ states which have an avoided crossing at ∼2.5 Å, which corresponds to $v \approx 4$ of the A state. The nonadiabatic coupled equations have been solved for this two-state interaction after constructing the diabatic potentials including only the diagonal ($\Delta\Lambda = 0$) spin-orbit coupling, yielding low-lying vibrational energy levels, isotope splittings, and rotational constants in good agreement with experiment. The calculations show that many of the observed bands are actually transitions to predominantly B state vibrational levels, which borrow oscillator strength from the A–X transition through spin-orbit mixing. Starting from the coupled equations solutions, we have fitted the experimental data using an effective Hamiltonian matrix that includes the vibrational energy levels of the A and B states and a single electronic spin-orbit coupling term H_{SO}^{AB} which has a value of 240 cm^{-1}. Transitions up to $v' = 32$ in both states have been satisfactorily fitted for all three chlorine isotopologues, providing a quantitative description of the perturbations. Transitions to higher levels are complicated by interactions with other electronic states. © *2012 American Institute of Physics*. [http://dx.doi.org/10.1063/1.4765334]

I. INTRODUCTION

The diatomic chlorine cation (Cl_2^+) is known to be produced in discharges through molecular chlorine and exhibits an emission spectrum with a large number of red degraded, rotationally discrete bands extending from 640 to 340 nm. These bands were first studied by Uchida and Ota[1] in 1928 and subsequently by several authors[2–6] culminating in a very detailed investigation by Huberman[7] published in 1966. These early investigations showed that the transition is $^2\Pi_i$–$^2\Pi_i$, that the rotational structure of most of the bands is quite regular, and that the pattern of vibrational levels in the ground state is also very regular. However, the upper state vibrational levels are chaotic, with irregular vibrational intervals and non-systematic chlorine isotope effects that made it impossible to assign vibrational quantum numbers to the observed bands. Since the electronic transition follows $\Delta\Omega = 0$ selection rules, the values of the spin-orbit (SO) splittings in the combining states could not be determined from the optical data. Huberman[7] identified two band systems, system I (terminating on $X\,^2\Pi_{3/2g}$ levels) and system II (terminating on $X\,^2\Pi_{1/2g}$ levels) and speculated that the perturbations were due to a homogeneous ($\Delta\Omega = 0$) interaction between $A\,^2\Pi_{3/2u}$ and $^2\Delta_{3/2u}$ and $A\,^2\Pi_{1/2u}$ and $^2\Sigma^+_{1/2u}$ states.

After an almost 20 year hiatus, advances in supersonic expansion techniques and in computational methods motivated Tuckett and Peyerimhoff to re-examine the Cl_2^+ emission spectrum both experimentally and theoretically.[8] It was somewhat easier to differentiate between the $\Omega = 3/2$ and the $\Omega = 1/2$ bands in the molecular beam source and the authors concluded that Huberman's original assignments are probably correct. One hundred vibronic bands were fitted into two Deslandres tables, one for $A\,^2\Pi_{3/2u}$–$X\,^2\Pi_{3/2g}$ transitions and one for $A\,^2\Pi_{1/2u}$–$X\,^2\Pi_{1/2g}$ transitions, accounting for over 80% of the observed bands. Unfortunately, vibrational quantum numbers were still not assignable despite a great deal of effort.

Ab initio theory[8] indicated that the $A^2\Pi_u$ state, formed by a $\pi_u \rightarrow \pi_g^*$ electron promotion from the $\ldots\ \sigma_g{}^2\ \pi_u{}^4\ \pi_g^{*3}$ $X\,^2\Pi_g$ ground state is energetically very close to the $^2\Sigma_u^-$, $^2\Sigma_u^+$, $^4\Sigma_u^-$, and $^2\Delta_u$ states derived from the $\ldots\ \sigma_g{}^2\ \pi_u{}^4\ \pi_g^{*2}$

a)Author to whom correspondence should be addressed. Electronic mail: dclaser@uky.edu.

σ_u^{*1} excited electron configuration. The authors concluded that homogeneous ($\Delta\Omega = 0$) perturbations between $B\ ^2\Delta_{3/2u}$ and $A\ ^2\Pi_{3/2u}$ and between $^2\Sigma^+{}_{1/2u}$ and $A\ ^2\Pi_{1/2u}$ levels with very similar bond lengths were the likely cause of the vibrational irregularities in the A state.

Five years later in 1989 Choi and Hardwick[9] obtained high resolution emission spectra of Cl_2^+ from a corona-excited supersonic expansion and identified four bands that exhibited Λ-doubling and could be unambiguously assigned as $A\ ^2\Pi_{1/2u}$–$X\ ^2\Pi_{1/2g}$. They agreed that Huberman's original ground state vibrational assignments were correct but could not provide any further information on the upper state vibrational numbering. In a subsequent paper,[10] they rotationally analyzed 15 bands with $\Omega = 3/2$ in both states, 10 of which were assigned to the $A\ ^2\Pi_{3/2u}$–$X\ ^2\Pi_{3/2g}$ band system analyzed by Huberman and 5 with somewhat smaller rotational constants which were assigned to perturbation-induced transitions whose most plausible assignment is $B\ ^2\Delta_{3/2u}$–$X\ ^2\Pi_{3/2g}$.

In 1990, Bramble and Hamilton[11] reported the first laser-induced fluorescence spectra of chlorine cation and measured single vibronic level (SVL) fluorescence lifetimes. The ions were produced in a pulsed supersonic discharge jet and all of the observed bands were assigned as originating from the $X\ ^2\Pi_{3/2g}$ component of $v'' = 0$. Two of their observations are very significant: six new bands not previously seen in any emission spectra were identified and found to have smaller B' values than previously observed transitions, and the fluorescence lifetimes were found to be vibronic level dependent, with longer values for the new bands. The authors argued that the direct absorption transition from the ground state to the perturbing $B\ ^2\Delta_{3/2u}$ or $^4\Sigma^-{}_{3/2u}$ electronic states is at least partially forbidden, accounting for the longer lifetimes of the mixed states.

The results of these last two studies, published contemporaneously, suggest that the matrix elements for the vibrational perturbations are of the order of magnitude of the excited state vibrational frequency (350–400 cm^{-1}) and most likely involve interactions with levels of the $B\ ^2\Delta_u$ excited state. Such perturbations would be expected to cause substantial vibrational irregularities in the A–X band system and generate interloper transitions through the mixing of the $A\ ^2\Pi_u$ and $B\ ^2\Delta_u$ levels.

In addition to emission and laser induced fluorescence (LIF) studies, photoelectron spectroscopy has contributed to our understanding of the chlorine cation.[12–18] In their high resolution UV photoelectron study, Van Lonkhuyzen and De Lange[15] obtained a value of $T_0 = 20648 \pm 400$ cm^{-1} and $A_{SO} = -550 \pm 100$ cm^{-1} for the A state. Yencha and coworkers[17] used threshold photoelectron spectroscopy to obtain the excited A state parameters $T_0 = 20382 \pm 35$ cm^{-1} and $A_{SO} = -790$ cm^{-1}. In recent ZEKE work, Li and coworkers[18] determined the spin-orbit splitting of the ground state to be -717.7 ± 1.5 cm^{-1}, and vibrational constants of $\omega_e = 646.9$ cm^{-1} and $\omega_e x_e = 3.15$ cm^{-1} for the lowest six levels of the $X\ ^2\Pi_{3/2g}$ spin-orbit component, confirming Huberman's ground state vibrational numbering.[7]

In the present work, we have generated very cold chlorine cations in a pulsed discharge jet and studied their LIF and emission spectra. The LIF spectra extend to much lower energy than previous studies and allow us to assign upper state vibrational quantum numbers with confidence for the first time. Our *ab initio* studies have clarified the nature and magnitude of the perturbations, culminating in an effective Hamiltonian least squares analysis of the observed transitions, yielding excited state molecular constants, perturbation matrix elements, and definitive vibrational assignments.

II. EXPERIMENT

The jet cooled chlorine cation (Cl_2^+) was produced using the pulsed electric discharge technique.[19,20] A precursor gas mixture of 5% chlorine gas (High purity, Matheson Tri-Gas) in argon (High purity, Scott Gross) was prepared in a stainless steel cylinder equipped with a pressure regulator to deliver a constant 40 psi pressure. Pulses of the precursor mixture were injected into a vacuum chamber through the 0.8 mm orifice of a pulsed solenoid valve (General Valve Series 9). After an appropriate time delay, an electric discharge was struck between two ring electrodes mounted in a Delrin cylinder attached to the face plate of the pulsed valve and along the path of the expanding gases.

Low resolution LIF spectra (0.1 cm^{-1}) of Cl_2^+ were collected in the 500–312 nm region by intercepting the expanding discharge products with the collimated beam of a pulsed, tunable excimer pumped dye laser (Lumonics HD 500). The resulting LIF was imaged through appropriate cutoff filters onto the photocathode of a high-gain photomultiplier tube (EMI 9816QB). Since the ions tend to have higher velocities than neutral molecules due to the space-charge effect (electrostatic repulsion), the optimum signal was obtained by using a relatively short time delay between the laser pulse and the electric discharge. The spectra were calibrated to an estimated accuracy of 0.1 cm^{-1} with optogalvanic lines of neon- and argon-filled hollow cathode lamps.

Single vibronic emission spectra were obtained by fixing the laser on an intense feature of a particular vibronic band and focusing the resulting fluorescence onto the entrance slit of a 0.5 m scanning monochromator (Spex 500M) equipped with an 1800 line/mm grating blazed at 400 nm. The dispersed emission was detected by a cooled photomultiplier (RCA C31034A). The monochromator was calibrated using the emission lines of an argon hollow cathode lamp to an accuracy of ± 1.0 cm^{-1}. Pulsed LIF or emission signals from the detectors and the optogalvanic apparatus were sampled with gated integrators and recorded digitally using a LabVIEW based data acquisition system.

High resolution (0.03 cm^{-1}) LIF spectra of selected bands of the $^{35}Cl_2^+$ and $^{35}Cl^{37}Cl^+$ isotopologues were obtained using a Lambda-Physik dye laser (Scanmate 2E) equipped with an intracavity angle-tuned etalon. In order to separate overlapping bands of the two isotopologues, the synchronous scan (sync-scan) LIF technique described in more detail in Ref. 21 was used. In this method, a monochromator, synchronously scanned with the LIF excitation laser, is used as a narrow bandpass filter to selectively detect one emission band from a single isotopologue. These spectra were calibrated using the I_2 LIF Raman shifting technique[22] to an estimated accuracy of ± 0.003 cm^{-1}.

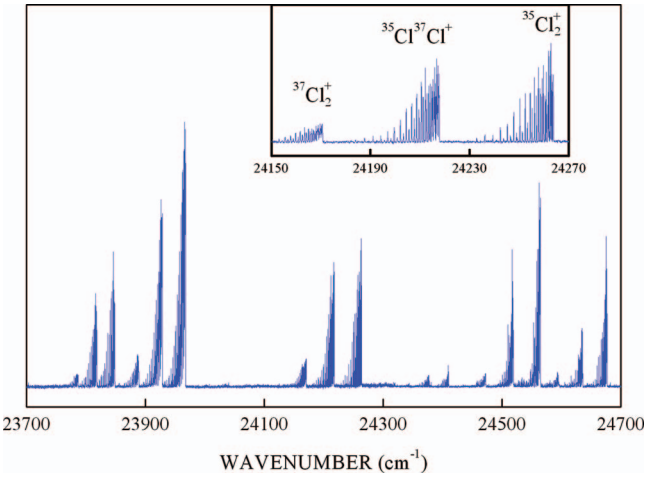

FIG. 1. A portion of the medium resolution LIF spectrum of jet-cooled chlorine cation showing the perturbed vibrational structure. The inset shows the chlorine isotope splittings and partially resolved rotational structure for one band.

III. RESULTS AND ANALYSIS

A. Description of the spectra

We began our experiments in the 400 nm region, which produced very strong LIF signals of chlorine cation. The spectra exhibit red-degraded bands with simple *P*, *Q*, and *R* branches and readily distinguished chlorine isotope structure as shown by the example in Fig. 1. The cold, unperturbed spectrum of a simple diatomic molecule should consist of a series of regularly spaced bands with a smooth intensity profile. In contrast, this spectrum, which includes some of the lowest energy cold bands identified in previous studies, shows many of the complications evident in the Cl_2^+ band system. The vibrational intervals are highly irregular and there are weaker interloper bands. Although the chlorine isotope splittings do not follow the expected regular patterns, they generally increase with excitation energy and the rotational structure of the bands appears largely unperturbed.

The spectra are exceptionally clean with very high signal-to-noise ratios and no evidence of extraneous signals from other molecules ($^{35}Cl_2$ is predissociated[23] above 19943.4 cm^{-1}). Since the isotope splittings are substantial (45−55 cm^{-1}) in this region of the spectrum, the 0-0 band is clearly to lower energy, so we extended our scan region progressively to the red where the bands get weaker and weaker, culminating in a very weak feature at 20286.0 cm^{-1}. This band is some 3700 cm^{-1} to lower energy than any previous absorption, LIF or emission cold band reported in the literature. Despite considerable effort, we were unable to detect any cold bands to lower frequencies. A summary of the data is presented in Table I.

The segment of the LIF spectrum in the lowest frequency region is shown in the top panel of Fig. 2 with the bands labeled 1−12 as in Table I. It is readily apparent that bands 1−4 appear largely unperturbed, with regular vibrational intervals and isotope shifts and no extraneous features. The interval between bands 4 and 5 is smaller than expected and two weaker interloper bands appear just above band 5, indicating the onset of the vibrational perturbations. Before discussing the assignments it is necessary to establish the degree of vibrational and spin-orbit cooling in our spectra.

Using the $v'' = 1 - v'' = 0$ interval of 640 cm^{-1} obtained from our own emission spectrum measurements (*vide infra*), we searched our LIF spectra for any evidence of hot bands, with no success, suggesting that all observed bands are vibrationally cold. As a test of this hypothesis, we altered the expansion conditions by adding a short reheat tube[24] and manipulating the time delay between the discharge and the laser for less efficient cooling and obtained the spectrum shown in the bottom panel of Fig. 2. A series of weak bands are observed which can be readily assigned as hot bands originating from $v'' = 1$ and 2, confirming that spectra obtained under the coldest expansion conditions have insignificant populations in $v'' > 0$.

The other obvious question concerns the extent of the spin-orbit cooling in our experiments. The ground state spin-orbit interval[18] is 717.7 ± 1.5 cm^{-1}, some 77 cm^{-1} higher than the vibrational fundamental, so it might be anticipated that the $v'' = 0$ $X\ ^2\Pi_{1/2g}$ level should be depopulated in the expansion. However, it is known that spin-orbit components sometimes cool rather inefficiently, so this is not *a priori* a necessarily good assumption. Initially, we attempted to find bands in our spectra that were known from previous work (vibrational and rotational analyses) to be $\Omega = 1/2 - \Omega = 1/2$ transitions, but were unable to identify any such features. We then attempted to differentiate the bands on the basis of low-resolution band contours, as shown in Fig. 3. The bottom trace is the experimental 0.15 cm^{-1} resolution spectrum of a $^{35}Cl_2^+$ band at 23249.2 cm^{-1} which we have analyzed as a transition between $^2\Pi_{3/2}$ spin-orbit components. The simulated spectrum is given in the central trace and the upper trace shows the corresponding $^2\Pi_{1/2}$ component calculated using the same *B* values but with the 8−1 band Λ-doubling constants determined by Choi and Hardwick.[9] We conclude that any $^2\Pi_{1/2}$ bands exhibiting Λ-doubling should be readily apparent at low-resolution. No such bands have been found in our spectra.

We have obtained approximate upper state *B* values for most of the low-resolution bands in the spectrum by band contour analysis using the very convenient graphical program PGOPHER.[25] In each case, we fixed $B'' = 0.2686$ cm^{-1} (from Ref. 7) and varied T_0 and B' until a good visual match was obtained between the observed and calculated partially resolved rotational structure. Comparisons between the *B* values determined in this fashion and the more accurate constants obtained for the same upper state levels by previous workers showed agreement out to the third decimal place, sufficient for the purposes of this work. The *B* values are summarized in Table I.

We have studied bands 2 and 3 (Fig. 2) at high resolution in order to unambiguously confirm that they involve the $^2\Pi_{3/2}$ spin-orbit components. Although these bands are weak, the use of the LIF sync-scan method provides spectra with excellent signal-to-noise ratio and no isotopic contamination, as shown in Fig. 4. Analysis clearly indicates that the lowest J'' values of both bands are 1.5, with no evidence of Λ-doubling, precisely as expected for $^2\Pi_{3/2}$ transitions. We have

TABLE I. Observed LIF band heads (cm^{-1}) of the Cl_2^+ isotopologues (relative intensities and rotational constants are for the $^{35}Cl_2^+$ species).

	Band Heads				Isotope shifts		Rotational constant B′	
Band #	$^{35}Cl_2^+$	$^{35}Cl^{37}Cl^+$	$^{37}Cl_2^+$	Intensity[a] ($^{35}Cl_2^+$)	$^{35}Cl_2^+$–$^{35}Cl^{37}Cl^+$	$^{35}Cl_2^+$–$^{37}Cl_2^+$	$^{35}Cl_2^+$	Upper state assignment
1	20286.0	20287.7	…	vw	−1.7	…	…	A; v = 0
2	20662.8	20659.5	…	vw	3.3	…	0.19123	A; v = 1
3	21031.1	21023.1	…	vw	8.0	…	0.18929	A; v = 2
4	21382.9	21371.2	…	vw	11.7	…	0.186	A; v = 3
5	21681.3	21670.4	…	vw	10.9	…	0.179	A; v = 4
6	21872.5	21865.4	…	vw	7.1	…	0.179	B; v = 0
7	21973.5	21966.7	…	vw	6.8	…	0.170	B; v = 1
8	22200.0	22180.6	22160.7	w	19.4	39.3	0.1788[b]	A; v = 5
9	22495.5	22474.0	22451.4	w	21.5	44.1	0.1729[b]	A; v = 6
							0.1733[c]	
10	22620.8	22607.0	…	vw	13.8	…	0.171	B; v = 3
11	22787.6	22768.7	22748.4	vw	18.9	39.2	0.1669[c]	B; v = 4
12	22942.3	22916.3	22890.5	ms	26.0	51.8	0.1749[b]	A; v = 7
13	23083.8	23067.3	…	vw	16.5	…	0.161	B; v = 5
14	23249.2	23215.6	23181.5	s	33.6	67.7	0.1742[b]	A; v = 8
							0.1744[c]	
15	23382.1	23362.6	…	vw	19.5	…	0.160	B; v = 6
16	23550.8	23516.5	23481.2	mw	34.3	69.6	0.1691[b]	A; v = 9
17	23675.6	23647.1	23618.3	mw	28.5	57.3	0.1653[c]	B; v = 7
18	23848.4	23818.2	23786.7	mw	30.2	61.7	0.161	B; v = 8
19	23967.1	23928.0	23888.6	vs	39.1	78.5	0.1690[c]	A; v = 10
							0.1694[b]	
20	24263.1	24217.6	24170.5	ms	45.5	92.6	0.1702[b]	A; v = 11
							0.1705[c]	
							0.1689[d]	
21	24410.1	24377.3	24343.7	vw	32.8	66.4	0.156	B; v = 10
22	24564.4	24519.1	24472.3	s	45.3	92.1	0.1664[b]	A; v = 12
							0.1659	
23	24676.7	24635.6	24594.5	ms	41.1	82.2	0.1588[c]	B; v = 11
							0.1596[d]	
24	24857.5	24817.6	24775.7	vw	39.9	81.8	0.157	B; v = 12
25	24947.1	24894.9	24845.6	mw	52.2	101.5	0.1641[b]	A; v = 13
							0.1638[c]	
							0.1640[d]	
26	25236.2	25179.6	25122.0	s	56.6	114.2	0.1665[b]	A; v = 14
							0.1669[c]	
27	25378.9	25334.4	25289.3	vw	44.5	89.6	0.156	B; v = 14
28	25532.5	25477.8	25422.0	s	54.7	110.5	0.1614[d]	A; v = 15
29	25625.0	25573.5	25522.1	ms	51.5	102.9	0.1541[d]	B; v = 15
30	25812.1	25764.0	25713.8	w	48.1	98.3	…	B; v = 16
31	25882.6	25820.3	25757.9	vs	62.3	124.7	0.1607[b]	A; v = 16
32	26058.3	26008.4	25957.7	vw	49.9	100.6	0.146	B; v = 17
33	26165.8	26101.1	26034.8	vs	64.7	131.0	0.1622[b]	A: v = 17
34	26289.0	26234.2	26179.2	vw	54.8	109.8	0.1451[d]	B; v = 18
35	26451.3	26389.4	26325.9	ms	61.9	125.4	0.157	A: v = 18
							0.1538[d]	
36	26519.3	26456.8	26395.0	mw	62.5	124.3	0.1491[d]	B; v = 19
37	26773.0	26701.2	26628.1	vs	71.8	144.9	0.1588[b]	A; v = 19
							0.1573[d]	
38	26928.3	26869.6	26809.0	vw	58.7	119.3	0.138	B: v = 21
39	27051.7	26980.1	26906.2	s	71.6	145.5	0.1568[b]	A; v = 20
40	27141.9	27078.5	27014.5	w	63.4	127.4	0.138	B; v = 22
41	27317.5	27289.1	27217.9	vw	28.4	99.6	0.145	B; v = 23
42	27362.6	27253.1	27184.3	s	109.5	178.3	0.148	A; v = 21
43	27535.0	27472.9	27408.7	vw	62.1	126.3	…	B; v = 24
44	27622.8	27544.6	27464.9	s	78.2	157.9	0.155	A; v = 22
45	27736.7	27670.5	27602.0	w	66.2	134.7	0.133	B: v = 25
46	27887.3	27812.6	27732.5	w	74.7	154.8	0.150	A; v = 23

TABLE I. (*Continued.*)

Band #	Band Heads $^{35}Cl_2^+$	Band Heads $^{35}Cl^{37}Cl^+$	Band Heads $^{37}Cl_2^+$	Intensity[a] ($^{35}Cl_2^+$)	Isotope shifts $^{35}Cl_2^+$–$^{35}Cl^{37}Cl^+$	Isotope shifts $^{35}Cl_2^+$–$^{37}Cl_2^+$	Rotational constant B′ $^{35}Cl_2^+$	Upper state assignment
47	27935.5	27864.1	27792.5	w	71.4	143.0	0.134	B; v = 26
48	28168.5	28086.8	28002.1	mw	81.7	166.4	…	A; v = 24
49	28297.9	28228.7	…	vw	69.2	…	0.129	B; v = 28
50	28425.1	28343.9	28260.5	w	81.2	164.6	0.149	A; v = 25
51	28482.5	28410.3	…	vw	72.2	…	0.129	B; v = 29
52	28691.8	28606.6	28518.4	w	85.2	173.4	0.149	A; v = 26
53	28823.5	…	…	vw	…	…	…	B; v = 31
54	28936.1	28852.3	28764.0	w	83.8	172.1	0.145	A; v = 27
55	28996.4	28922.5	…	mw	73.9	…	0.123	B; v = 32
56	29189.9	29101.5	29014.0	mw	88.4	175.9	0.143	A; v = 28
57	29420.9	29335.6	29246.1	mw	85.3	174.8	…	A; v = 29
58	29474.6	29400.4	29315.7	w	74.2	158.9	…	…
59	29660.7	29571.1	29480.3	mw	89.6	180.4	0.140	A; v = 30
60	29880.8	29794.3	29703.4	w	86.5	177.4	0.140	A; v = 31
61	29915.6	29841.2	29769.5	vw	74.4	146.1	0.114	…
62	30104.3	30015.3	29923.3	w	89.0	181.0	0.135	A: v = 32
63	30245.2	30184.1	…	vw	61.1	…	0.110	…
64	30322.9	30224.5	30134.7	w	98.4	188.2	0.124	A; v = 33[e]
65	30517.0	30421.0	30337.7	w	96.0	179.3	0.121	A; v = 34
66	30724.9	30644.3	…	w	80.6	…	0.124	A; v = 35
67	30921.8	30835.4	30736.6	w	86.4	185.2	0.120	A; v = 36
68	31106.8	…	…	w	…	…	…	A; v = 37
69	31280.0	31190.3	…	w	89.7	…	…	A; v = 38
70[f]	31439.4	31354.9	…	w	84.5	…	…	A; v = 39

[a]vw: very weak, w: weak, mw: medium to weak, ms: medium to strong, s: strong, vs: very strong.
[b]From Ref. 7.
[c]From Ref. 10.
[d]From Ref. 11.
[e]This and subsequent assignments are tentative as these bands have not been fitted with the effective Hamiltonian model; see text.
[f]Further weak bands that could not be assigned to a particular chlorine isotopologue or vibrational level were measured at 30455.8, 30471.8, 30490.3, 30561.2, 30576.2, 30789.1, 30885.0, 30989.2, 31014.2, 31026.1, 31175.1, 31206.4, 31288.4, 31367.8, 31489.5, 31513.0, 31561.2, 31585.4, 31621.9, 31647.0, 31691.7, 31710.4, 31734.0, 31756.2, 31794.7, 31806.3, 31837.6, 31868.7, 31898.4, and 31929.4 cm^{-1}.

used PGOPHER[25] to fit the individual rovibronic transitions using least squares methods. In each case, we were able to fit the rotational structure, which is free of detectable perturbations, to experimental accuracy (0.003 cm^{-1}) by varying only T_0, B'', and B', with the results shown in Table II. The ground state B values are the same within their respective uncertainties (average = 0.2686 cm^{-1}) and identical to that ob-

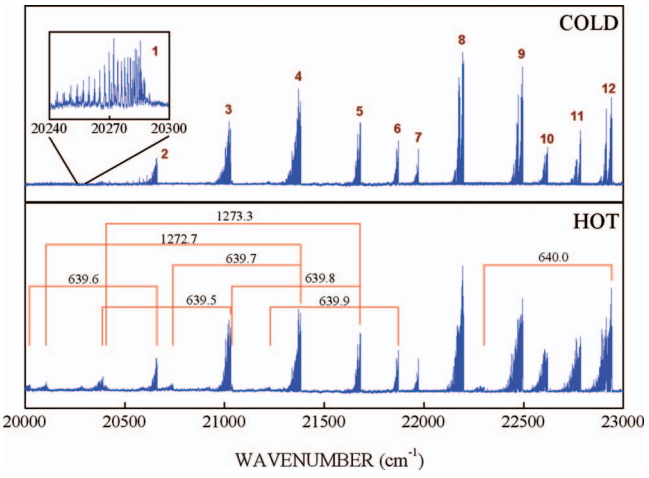

FIG. 2. The low energy end of the LIF spectrum of chlorine cation. The top "cold" spectrum was taken under expansion conditions that maximize the ground state vibrational and spin-orbit cooling. All the observed transitions in this spectrum originate in the v″ = 0 level of the lowest Ω = 3/2 spin-orbit component of the $X\,^2\Pi_g$ state. The inset shows the very weak 0–0 band. The bottom "hot" spectrum was recorded under much less vigorous cooling conditions and exhibits hot bands arising from v″ = 1 and v″ = 2.

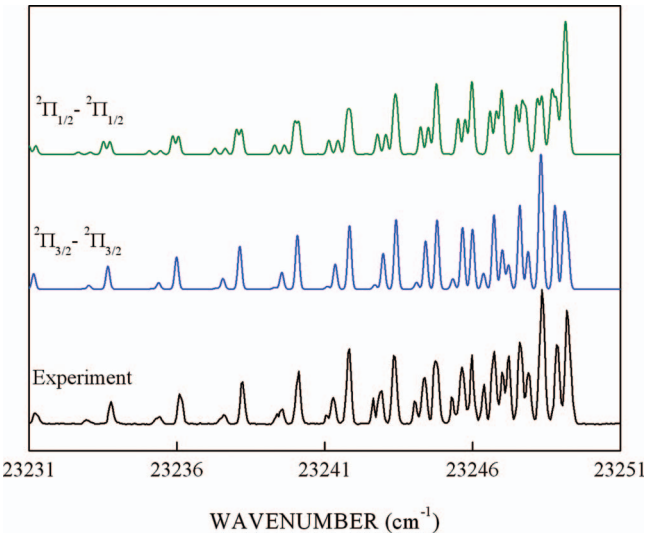

FIG. 3. A comparison of the rotational contour of an observed Cl_2^+ band and calculated contours for Ω = 1/2 (top) and 3/2 (middle) transitions.

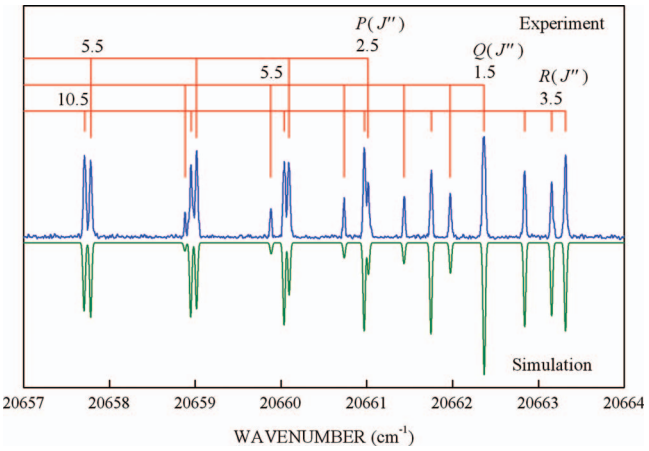

FIG. 4. A portion of the high-resolution $^{35}Cl_2^+$ 1–0 band sync-scan LIF spectrum with rotational assignments. The overlapping $^{35}Cl^{37}Cl^+$ lines present in the total LIF spectrum are completely suppressed here. The bottom trace shows the PGOPHER simulation using the constants in Table II and a rotational temperature of 30 K.

tained for v″ = 0 by Huberman,[7] indicating that both bands originate from the same ground state v″ = 0 $X\,^2\Pi_{3/2g}$ level. The excited state B values are larger than any of those determined in the early literature and almost identical to those obtained recently from analyses of the $^2\Pi_{1/2}$ bands at 16 913 and 17 282 cm^{-1}, tentatively assigned as 2−7 and 3−7.[26] We are led to the definite conclusion that all the bands in our cold spectra originate in the ground state v = 0 $X\,^2\Pi_{3/2g}$ level.

In addition to LIF spectra, we also obtained wavelength resolved emission spectra for many upper state levels. By laser excitation of higher energy LIF bands where the chlorine isotopologues are completely resolved, we have recorded emission spectra of $^{35}Cl_2^+$, $^{35}Cl^{37}Cl^+$, and $^{37}Cl_2^+$. Combining the data from several such spectra, we have mapped out the ground state energy levels and determined the vibrational constants of the three isotopologues, as presented in Table III.

B. Determination of the vibrational numbering of the lowest LIF bands

The crucial question for a band system with such a long Franck-Condon profile is what is the upper state vibrational assignment of our lowest cold band with band head at 20286.0 cm^{-1}? Is it the 0−0 band or are there more bands, too weak to be detected, to lower energies? Unfortunately, this band has very low intensity and we were unable to subject it to a detailed rotational analysis or obtain emission spectra from it.

TABLE II. The rotational constants (in cm^{-1}) of $^{35}Cl_2^+$ and $^{35}Cl^{37}Cl^+$.

	1–0 band		2–0 band	
Constant[a]	$^{35}Cl_2^+$	$^{35}Cl^{37}Cl^+$	$^{35}Cl_2^+$	$^{35}Cl^{37}Cl^+$
B''	0.26864(10)[b]	0.26139(10)	0.26863(15)	0.26145(14)
B'	0.19123(9)	0.18611(9)	0.18929(13)	0.18430(12)
T_0	20625.844(3)	20622.580(3)	20994.118(3)	20986.134(3)

[a]The spin-orbit coupling constants were fixed at $A' = -790$ cm^{-1} (Ref. 17) and $A'' = -717.7$ cm^{-1} (Ref. 18).
[b]The numbers in parentheses are standard errors of 3σ.

TABLE III. Measured ground state $^2\Pi_{3/2g}$ energy levels, the fitted vibrational constants, and the least squares residuals (all in cm^{-1}), from the emission spectra of $^{35}Cl_2^+$, $^{35}Cl^{37}Cl^+$, and $^{37}Cl_2^+$.

	$^{35}Cl_2^+$		$^{35}Cl^{37}Cl^+$		$^{37}Cl_2^+$	
v	Energy[a]	Residual	Energy	Residual	Energy	Residual
1	640	0.3	632	−0.1	623	0.2
2	1273	−0.1	1258	0.1	1240	−0.5
3	1901	0.3	1877	−0.8	1852	-0.3
4	2522	−0.4	2493	1.2	2459	0.8
5	3138	−0.2	3100	0.0	3059	0.6
6	3748	−0.1	3702	−0.3	…	…
7	4352	−0.2	4298	−0.7	4239	−2.1
8	4951	0.6	4889	−0.2	4826	2.3
9	5542	−0.7	5475	1.2	5399	−1.5
10	6129	−0.2	6052	−0.6	5972	0.6
11	6710	0.2	…	…	…	…
12	7285	0.5	…	…	…	…
13	7854	0.7	…	…	…	…
14	8416	−0.3	8309	0.0	…	…
15	8973	−0.4	…	…	…	…
ω_e	645.15(12)[b]		637.54(23)		629.31(70)	
$\omega_e x_e$	2.9345(69)		2.938(14)		2.919(57)	

[a]Energy above the lowest vibrational level of the $X\,^2\Pi_{3/2g}$ state.
[b]The numbers in parentheses are standard errors of 1σ.

However, chlorine isotope effects strongly indicate that it is in fact the 0–0 band. From the high resolution analyses, we obtain the precise $^{35}Cl_2^+ - ^{35}Cl^{37}Cl^+$ isotope shifts of bands 2 and 3 as +3.26 and +7.98 cm^{-1} and band 1 has an isotope effect estimated from band heads as −1.7 cm^{-1}. Using our ground state vibrational constants from SVL emission spectra of $\omega_e = 645.0$ cm^{-1} and $\omega_e x_e = 2.93$ cm^{-1} and an estimated range of upper state constants of ω_e = 350–400 cm^{-1} with $\omega_e x_e = 2.0$ cm^{-1}, the 0–0 band isotope shift is readily calculated to be from −2.0 to −1.7 cm^{-1}. The calculated isotope shifts for the 1−0 and 2−0 bands are *positive* with values of 2.7−3.7 cm^{-1} and 7.2−8.9 cm^{-1}, very similar to the observed values of bands 2 and 3 in our LIF spectra. A consistent picture emerges with bands 1, 2, and 3 assigned as 0−0, 1−0, and 2−0, respectively. The only caveat is that the higher bands in the spectrum are known to be perturbed with irregular isotope splittings which cannot be relied on to determine the vibrational numbering.

The final piece of evidence concerning the vibrational numbering comes from SVL emission spectra. The emission spectra from bands 2−5 (see Fig. 2) are shown in Fig. 5. It is well known that the number of nodes in such dispersed fluorescence spectra should be the same as the upper state vibrational quantum number and it is apparent that the lowest frequency LIF band 2 has an emission spectrum with *at least* one node. Unfortunately, we have no method to tell whether there is a second node as the spectrum extends beyond the range of our monochromator/detector limit of 850 nm. It is also evident that going to higher upper state quantum numbers (bands 3–5) shifts the Franck-Condon pattern in a systematic way suggesting that the upper state wavefunctions are not heavily perturbed and the number of nodes is still a useful, although in this case experimentally limited, diagnostic. We conclude that the existence of one node argues strongly

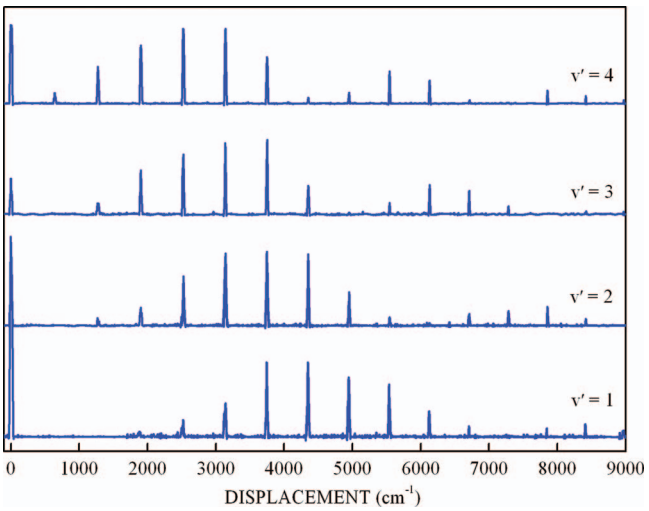

FIG. 5. Single vibronic level emission spectra obtained by laser excitation of bands 5 (top) to 2 (bottom) (see Fig. 2) in the LIF spectrum of chlorine cation. In each case the horizontal scale is displacement from the laser excitation wavenumber, which gives a direct measure of the ground state energy relative to that of $v'' = 0$. The feature at 0.0 cm^{-1} is scattered laser light.

that the upper state of cold band 2 is $v' = 1$, in accord with the isotope data.

With the LIF bands 1–3 established as transitions to $v' = 0$, 1, and 2, respectively, we can now examine the higher energy bands listed in Table I and attempt to make vibrational assignments. The first four bands (0−0, 1−0, 2−0, and 3−0) appear fairly regular with vibrational intervals of 377, 369, and 352 cm^{-1} and isotope shifts of −1.7, 3.3, 8.0, and 11.8 cm^{-1} although the 3−0 isotope splitting is slightly smaller than calculated (11.6–14.0 cm^{-1}) and the anharmonicity is quite a bit larger than that of the ground state. Curiously, the B_v values of bands 2–4 fit very well with the usual relationship yielding $B_e = 0.1953(9)$ cm^{-1} and $\alpha_e = 0.0026(4)$ cm^{-1}. In attempts to assign the 4−0 band, we confront an immediate problem, as there are three weak bands (labeled 5, 6, and 7 in Fig. 2) in the vicinity, all with isotope effects smaller than expected. Undoubtedly, some of these bands are transitions to the interloper states that perturb the $A\ ^2\Pi_{3/2u}$ levels. Using the data in Table I and the previously noted criterion that the B values of the interloper states are significantly smaller than those of A state levels, it appears that band 7 terminates on an interloper state with $B' = 0.170$ cm^{-1}. Bands 5 and 6 have anomalously small isotope effects (10.9 and 7.1 cm^{-1}), B' values (0.179 and 0.179 cm^{-1}), and vibrational intervals (298 and 191 cm^{-1}) and it proved difficult to assign them with any certainty. These difficulties only increase as one moves to higher bands in the spectrum. At this point, we appealed to theory to attempt to understand the nature of the perturbations in more detail, which would hopefully allow us to make definitive assignments for the observed bands.

IV. COMPUTATIONAL DETAILS

A. *Ab initio* electronic structure calculations

For the description of the Cl atom, the correlation consistent polarized valence quadruple zeta basis set augmented by a large exponent d function (cc−pV(Q+d)Z) (16*s*11*p*4*d*2*f*1g)[27] was employed, generally contracted to [6*s*5*p*4*d*2*f*1g], giving a total of 64 spherical Gaussian functions.

Our zeroth-order wavefunctions are of a complete active space self-consistent field (CASSCF) type constructed by distributing all 13 valence electrons into 8 molecular orbitals correlating to the atomic 3*s*+3*p* valence shell. A state average (SA) treatment for states of the same spin and spatial ($\pm\Lambda$) symmetry was used under D_{2h} symmetry and equivalence restrictions. This way all molecular $|\Lambda S\rangle$ states dissociate smoothly to their respective adiabatic fragments at the Hartree-Fock limit. Additional correlation was extracted by single and double replacements out of all configuration functions (CF) of the reference CASSCF space (CASSCF+1+2 = MRCI). The resulting configuration interaction (CI) spaces (∼1.5 × 10^6 CFs) were subsequently internally contracted (*ic*MRCI) to approximately 1/4 of their initial size. We have thus constructed complete potential energy curves (PEC) for all the Cl_2^+ states of $^{2,4}(\Sigma^+,\ \Sigma^-\ [2],\ \Pi\ [2],\ \Delta)_{g,u}$ symmetry, dissociating adiabatically to the ground state atomic fragments $Cl(3s^23p^5;\ ^2P) + Cl^+(3s^23p^4;\ ^3P)$ (see Fig. 6). Size non-extensivity errors are mitigated through the multireference analog of the Davidson correction, denoted as +Q in what follows.[28] The molecular constants and other relevant features of the bound state PEC's are summarized in the accompanying supplementary material.[29]

Spin-orbit coupling has been accounted for by diagonalizing the $H_{el} + H_{SO}$ in a basis comprising the eigenfunctions of the electronic Hamiltonian H_{el}. The full Breit-Pauli operator is used for the calculation of the matrix elements between the CFs of the "internal" zeroth-order CASSCF wavefunction, while the effect of the "external" space is considered through a mean field one-electron Fock operator.[30]

Since we are only interested in deciphering the $A\ ^2\Pi_{3/2u}$–$X\ ^2\Pi_{3/2g}$ Cl_2^+ spectrum, we had to adjust our SO computational strategy accordingly. We have obtained the lower state PEC by diagonalizing the SO operator within a space comprising only the 4 $\Lambda+\Sigma$ (= Ω) components of the $X\ ^2\Pi_g$ state. The upper $\Omega = 3/2_u$ states were obtained from a 16 × 16 matrix generated by all Ω components of the $^4\Sigma_u^-$, $^2\Pi_u$, $^2\Delta_u$, $^2\Sigma_u^+$, and $^2\Sigma_u^-$ states. The presence of the latter two $\Lambda = 0$ states in the SO matrix is important since their $\Omega = 1/2_u$ components interact heavily with $A\ ^2\Pi_{1/2u}$ (see Fig. 7). Our basis set is well suited for such a computational endeavor. For example, the ionization energy (IE) of the Cl atom is found to be IE = 12.73 (12.84) eV at the CISD(+Q) level of theory and compares nicely with the experimental value of 12.9676 eV.[31] The atomic SO splittings of both the neutral $Cl(^2P)$ and ionic $Cl^+(^3P)$ atoms [$\Delta E_{Cl}(1/2-3/2) = 794.45$ cm^{-1}, $\Delta E_{Cl}^+(1-2) = 605.80$ cm^{-1}, and $\Delta E_{Cl}^+(0-2) = 908.71$ cm^{-1}] also compare well with the experimental values of 882.35, 696.00, and 996.47 cm^{-1}, respectively.[32]

For all electronic structure calculations, the MOLPRO 2010.1 suite of programs was employed.[33]

B. Coupled equations

Figure 6 shows the PECs of all $|\Lambda S\rangle$ states dissociating to $Cl(3s^23p^5;\ ^2P) + Cl^+(3s^23p^4;\ ^3P)$ calculated at the

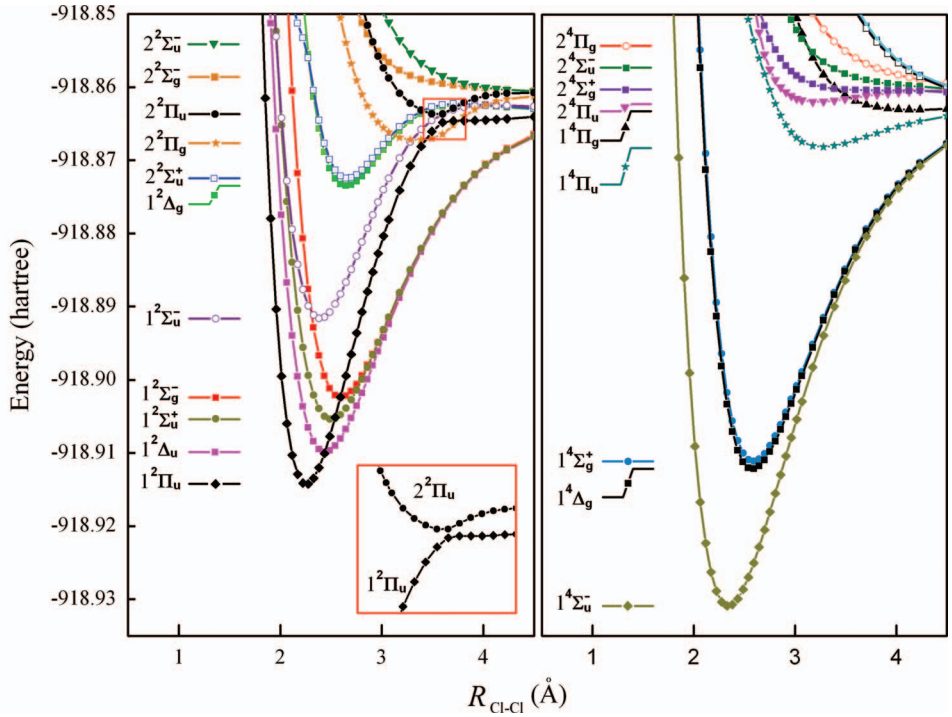

FIG. 6. The MRCI potential energy curves for the excited states of chlorine cation that dissociate to the ground state atomic fragments $Cl(3s^2 3p^5;\ ^2P) + Cl^+(3s^2 3p^4;\ ^3P)$.

MRCI level of theory. The $A\ ^2\Pi_u$ and $B\ ^2\Delta_u$ PECs cross at ~2.22 Å. When the spin-orbit interaction is considered, the crossing becomes avoided and the A and B states exchange their electronic character (see Fig. 7). It is this spin-orbit $\Delta\Omega = 0$ interaction that leads to the observed perturbations in the A–X band system of Cl_2^+. The main CASSCF equilibrium configurations of the B state are

$$\left|B^2\Delta_u\right\rangle \simeq 0.60\left|...\sigma_g^2\pi_u^4\sigma_u^1\pi_g^2\right\rangle - 0.37\left|...\sigma_g^2\pi_g^4\sigma_u^1\pi_u^2\right\rangle.$$

It is important to note that the spin-orbit interaction is not due to the main configurations of the A $(...\sigma_g^2\pi_u^3\pi_g^4)$ and $B(...\sigma_g^2\pi_u^4\sigma_u^1\pi_g^2)$ states, which differ by two spin orbitals, but due to the 0.37 component $(...\sigma_g^2\pi_g^4\sigma_u^1\pi_u^2)$ of the $B\ ^2\Delta_u$ state, as originally suggested by Bramble and Hamilton.[11]

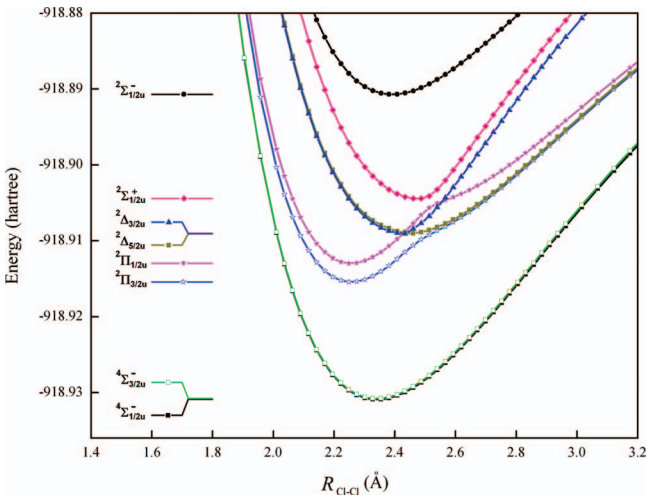

FIG. 7. Potential energy curves including the spin-orbit interaction for the lowest few u symmetry electronic excited state of chlorine cation. States of the same Ω value interact, leading to avoided crossings.

The state mixing results in the breakdown of the Born-Oppenheimer (BO) approximation, so that the vibronic levels should be found by solving the coupled equations.[34] It is well known (see p. 264 of Ref. 35) that their form depends on the choice of either diabatic or adiabatic electronic wavefunctions. In the present case, we can define in a natural way a diabatic basis comprised of the adiabatic MRCI PECs after the inclusion of the diagonal SO energy contribution. Since the $^4\Sigma^-_{3/2u}$ state is practically a pure quartet spin state (circa 99.5% of $^4\Sigma_u^-$ character at all R distances) the upper $\Omega = 3/2_u$ vibronic levels can be adequately approximated by a two BO term wavefunction

$$\psi_i(q, R) = \frac{1}{R}[\Phi_A^d(q; R)\chi_{A,i}^c(R) + \Phi_B^d(q; R)\chi_{B,i}^c(R)], \tag{1}$$

where q stands for the set of electronic coordinates, R for the internuclear distance, d for diabatic, and c for coupled.

The vibrational functions $\chi_{n,i}^c(R)$ are the solutions of the following nonadiabatic coupled equations:

$$[-(\hbar^2/2\mu)\frac{d^2}{dR^2} + V_A^d(R)]\chi_{A,i}^c(R) + H_{SO}^{AB}(R_c)\chi_{B,i}^c(R) = E_i\chi_{A,i}^c(R), \tag{2}$$

$$[-(\hbar^2/2\mu)\frac{d^2}{dR^2} + V_B^d(R)]\chi_{B,i}^c(R) + H_{SO}^{AB}(R_c)\chi_{A,i}^c(R) = E_i\chi_{B,i}^c(R). \tag{3}$$

TABLE IV. The results of the coupled equations calculations for the chlorine cation (in cm^{-1}). In each case Diff. denotes the experimentally observed value (see Table I) minus the calculated value.

Band origin		B'_v		Assignment		$^{35}Cl_2^+$–$^{35}Cl^{37}Cl^+$		$^{35}Cl_2^+$–$^{37}Cl_2^+$	
Calc.	Diff.	Calc.	Diff.	% *A*	% *B*	Calc.	Diff.	Calc.	Diff.
20285.9	0.1	0.1887	…	99 v = 0	1 v = 0	− 1.7	0.0	− 3.5	…
20658.4	4.4	0.1871	0.0041	98 v = 1	2 v = 0	3.2	0.1	6.5	…
21022.9	8.2	0.1853	0.0040	96 v = 2	4 v = 0	7.9	0.1	16	…
21373.5	9.4	0.1826	0.0034	91v = 3	9 v = 0	11.9	− 0.2	24	…
21682.3	− 1.0	0.1754	0.0036	66 v = 4	34 v = 0	12.1	− 1.2	24.8	…
21881.1	− 8.6	0.1711	0.0079	45 v = 4	55 v = 0	6.7	0.4	13.9	…
21990.1	− 16.6	0.1668	0.0032	31 v = 5	69 v = 1	6.9	− 0.1	13.5	…
22192.7	7.3	0.1746	0.0042	70 v = 5	30 v = 1	18.6	0.8	37.2	2.1
22314.0	…	0.1625	…	13 v = 6	87 v = 2	4.9	…	9.9	…
22491.2	4.3	0.1725	0.0008	68 v = 6	32 v = 2	23.3	− 1.8	47.3	− 3.2
22634.8	− 14.0	0.1640	0.0070	26 v = 6	74 v = 3	12	1.8	24.2	…
22794.8	− 7.2	0.1674	− 0.005	49 v = 7	51 v = 4	21.8	− 2.9	44.4	− 5.2
22938.2	4.1	0.1672	0.0077	50 v = 7	50 v = 4	22.9	3.1	45.7	6.1
23105.2	− 21.4	0.1612	− 0.0002	24 v = 8	76 v = 5	17.9	− 1.4	36.3	…
23233.4	15.8	0.1699	0.0043	70 v = 8	30 v = 5	32.5	1.1	65.9	1.8
23406.2	− 24.1	0.1574	0.0026	13 v = 9	87 v = 6	19	0.5	38.5	…
23536.0	14.8	0.1699	− 0.0008	75 v = 9	25 v = 6	36.5	− 2.2	73.8	− 4.2
23688.7	− 13.1	0.1573	0.0080	21 v = 10	79 v = 7	26.2	2.3	52.9	4.4
23849.8	− 1.4	0.1655	− 0.0045	58 v = 10	42 v = 8	34.3	− 4.1	69.9	− 8.2
23960.7	6.4	0.1597	0.0093	40 v = 10	60 v = 8	34.8	4.3	69.2	9.3

To solve them, we have used the Fox-Goodwin propagation scheme[36] with matching of propagated outward and inward solution matrices.[37] The number of integration points has been taken equal to 2001, with a grid extending from $R_{min} = 1.48$ Å to $R_{max} = 5.29$ Å. The only empirical adjustment is that the *B* state diabatic curve has been shifted upwards by 140 cm^{-1} in order to match experiment as closely as possible. We have obtained the vibronic levels and corresponding wavefunctions for the three isotopologues, $^{35}Cl_2^+(\mu$ = 17.48442634 amu), $^{35}Cl^{37}Cl^+$ (μ = 17.96982831 amu), and $^{37}Cl_2^+$ (μ = 18.4829513 amu). We have also calculated B'_i as an expectation value based on the following simple expression:

$$B'_i = \int_{R_{min}}^{R_{max}} (\hbar^2/2\mu R^2)\left(\chi^c_{A,i}(R)^2 + \chi^c_{B,i}(R)^2\right)dR. \quad (4)$$

Once the *i*th solution of Eqs. (2) and (3) was obtained, the nuclear factors $\chi^c_{n,i}(R)$ were normalized according to

$$\int_{R_{min}}^{R_{max}} \left[\chi^c_{A,i}(R)^2 + \chi^c_{B,i}(R)^2\right]dR = 1. \quad (5)$$

The percentage $P_{n,i}$ of each nuclear factor is given by

$$P_{n,i} = 100 \int_{R_{min}}^{R_{max}} \chi^c_{n,i}(R)^2 dR \quad (n = A, B). \quad (6)$$

We label the vibronic levels based on the largest percentage of a given diabatic state. The vibrational quantum numbers were determined by comparing plots of the associated nuclear wavefunctions $\chi^c_{n,i}$ to the shapes of the corresponding diabatic vibrational wavefunctions and identifying which functions were most similar.

C. Computational results

Figure 6 indicates four low-lying electronic states ($A\ ^2\Pi_u$, $B\ ^2\Delta_u$, $1^2\Sigma_u^+$, and $1^2\Sigma_u^-$) accessible by electronically allowed electric dipole transitions from the $X\ ^2\Pi_g$ state. However, our transition moment calculations show that the vertical transition to the *A* state is very strong ($R_{e'e''} = 1.8$ D), whereas transitions to the other states are much weaker ($B\ ^2\Delta_u = 0.07$ D, $1^2\Sigma_u^+ = 0.01$ D, and $1^2\Sigma_u^- = 0.16$ D), consistent with our observation that all the bands in our spectra have simple $\Delta\Lambda = 0$ rotational structure. Franck-Condon factors calculated for the *A*–*X* transition from the curves in Fig. 6 indicate a very weak 0–0 band, a long Franck-Condon profile, peaking at about v′ = 23 and tailing off to dissociation at about v′ = 42. Since our spectra contain about 100 bands (see Table I), many of the observed features must be perturbation-induced interloper bands.

The results of the solution of the coupled equations for the lower levels of the *A*–*X* transition are presented in Table IV. The agreement with experiment is very gratifying and clearly leads to definitive assignments. The first four levels are primarily v = 0–3 of the *A* state, perturbed slightly from above by interaction with energetically distant levels of the *B* state. The *A* state v = 4 level interacts strongly with the nearby v = 0 level of the *B* state, yielding bands 5 (66% *A* v = 4) and 6 (55% *B* v = 0) in the spectrum. Due to the lower vibrational frequency in the *B* state (286 cm^{-1} vs. 382 cm^{-1} in the *A* state), the levels interleave, producing interloper band 7 (69% *B* v = 1), and perturbed band 8 (70% *A* v = 5). Then the calculation predicts a band at 22314 cm^{-1} with upper state 87% *B* v = 2 that is not observed in the spectrum. This is reasonable because the mixing with the *A* state, which carries all the oscillator strength, is very small, so the interloper

	A v = 0	A v = 1	A v = 2	A v = 3	...	B v = 0	B v = 1	B v = 2	B v = 3	...
A v = 0	E(A v=0)					Symmetric				
A v = 1		E (A v=1)								
A v = 2			E (A v=2)							
A v = 3				E (A v=3)						
...					...					
B v = 0	X_{00}	X_{01}	X_{02}	X_{03}	...	E(B v=0)				
B v = 1	X_{10}	X_{11}	X_{12}	X_{13}	...		E(B v=1)			
B v = 2	X_{20}	X_{21}	X_{22}	X_{23}	...			E(B v=2)		
B v = 3	X_{30}	X_{31}	X_{32}	X_{33}	...				E(B v=3)	
...	...	...	...	...	...					...

FIG. 8. The form of the effective Hamiltonian matrix used to calculate the vibronic energy levels in the spectrum of Cl_2^+. The diagonal energy terms are just $E_v = T_e + \omega_e (v + 1/2) - \omega_e x_e (v + 1/2)^2 + \omega_e y_e (v + 1/2)^3 + \ldots$ and the off-diagonal terms X_{ij} are $H_{SO}^{AB} \langle \chi^d{}_{vA} | \chi^d{}_{vB} \rangle$.

band is undetectably weak. Turning to the calculated B values, it is evident that they are generally slightly smaller than the experimental values but follow the observed trend, with smaller values for the B state vibrational levels, consistent with the *ab initio* predictions: A state $R_e = 2.25$ Å and B state $R_e = 2.44$ Å. Finally, the data in Table IV also show that the calculations satisfactorily reproduce the chlorine isotope shifts for bands 1–8.

The calculations continue to match experiment very well until the last two entries in Table IV, which predict a perturbed band (58% A v = 10; 42% B, v = 8) at 23849.8 cm^{-1} with the larger B value and an interloper band (40% A v = 10; 60% B v = 8) above it at 23960.7 cm^{-1} with a smaller B value. However, the spectrum begs to differ, with the weaker interloper (with smaller B value) occurring at 23848.4 cm^{-1}, below the very strong perturbed band with larger B value at 23967.1 cm^{-1}. Clearly, the actual mixing of the A and B state wavefunctions is not quite as predicted by the calculations. At higher energies, the agreement between the observed and calculated properties of the spectrum slowly degrades, reflecting the limitations of a purely two-state *ab initio* model.

V. FITTING THE EXPERIMENTAL DATA

The coupled equations clearly show that the perturbations are due to a spin-orbit interaction between the $\Omega = 3/2$ components of the $A\ ^2\Pi_u$ and $B\ ^2\Delta_u$ electronic states. In order to treat the data more quantitatively, we have used an effective Hamiltonian with vibrational and spin-orbit interaction constants that could be refined by least squares methods. The matrix element coupling a level of the A state with vibrational quantum number v_A to a level of the B state with vibrational quantum number v_B can be written as $H_{SO}^{AB} \langle \chi^d{}_{vA} | \chi^d{}_{vB} \rangle$, where the first term is the electronic spin-orbit interaction matrix element and the second term is a vibrational overlap.[35] Our *ab initio* SO calculations showed that H_{SO}^{AB} has a value of about 240 cm^{-1} and that this value is almost constant (within 20%) from $R = 2.0$ to 3.6 Å. We obtained the preliminary vibrational overlaps (A state up to v = 42, B state up to v = 60, limited by dissociation) and vibrational constants from the MRCI PECs (Fig. 6).

A large matrix of the form shown in Fig. 8 was set up and diagonalized and the eigenvalues, eigenvectors, and derivatives were stored. The vibrational constants of each electronic state and the spin-orbit coupling term H_{SO}^{AB} were varied to minimize the sum of the squares of the deviations of the observed and calculated transition frequencies. The initial fitting was guided by the coupled equations calculation. Starting with the first 20 transitions of $^{35}Cl_2^+$ (see Table I, up to A v = 11, B v = 8), we found that we could obtain a good fit with a minimal set of constants, as long as the basis extended up to v = 30 for both electronic states. Examination of the *ab initio* vibrational overlaps of the A state v = 10 level, for example, showed that they range from 0.41 with B v = 4 to 0.11 with B v = 34, slowly dying off at higher levels, which accounts for the necessity of a large vibrational basis. Although the maximum interaction occurs between energetically similar levels, the large matrix elements [240 $cm^{-1} \times 0.41 = 98.4$ cm^{-1} at B v = 4 down to 26.4 cm^{-1} at B v = 34] mandate significant level shifts due to more remote levels as well.

In each case, we have fitted the band head data of Table I, rather than vibrational band origins which cannot be determined precisely without full rotational analysis. However, this introduces little error as tests show that the band origins are only 0.3–0.5 cm^{-1} to lower energy, well within the overall standard error for the least squares analysis.

Bootstrapping up from our initial set of $^{35}Cl_2^+$ assignments, we found that all of the A state levels up to v = 32 could be readily identified, along with most of the B state levels up to v = 32 (for some B state levels the mixing is too small to generate any appreciable intensity as found in the coupled equations calculations). In our initial analysis, we varied T_e, ω_e, $\omega_e x_e$, and $\omega_e y_e$ in both states and the single interaction constant H_{SO}^{AB}, using the *ab initio* vibrational overlaps. New PECs and vibrational overlaps were then calculated from the fitted vibrational constants using LeRoy's RKR1 2.0 and LEVEL 8.0 programs[38,39] and the process was repeated until no further improvements in the least squares fitting could be achieved. In this fashion, all the observed transitions of $^{35}Cl_2^+$ up to $v' = 32$ (85% of those in Table I) were fitted to an overall standard error of 0.7 cm^{-1}, about 1 order of magnitude larger than the measurement error, typical

TABLE V. The fitted[a] vibrational and spin-orbit interaction constants (in cm^{-1}) of Cl_2^+.

Constant	$^{35}Cl_2^+$	$^{35}Cl^{37}Cl^+$	$^{37}Cl_2^+$
	$A\,^2\Pi_{3/2u}$ state		
T_e	20440.81(72)	20441.53(70)	20440.81[b]
ω_e	386.46(36)	381.29(35)	376.24(17)
$\omega_e x_e$	2.027(47)	1.976(45)	1.944(16)
$\omega_e y_e$	−0.0299(21)	−0.0294(20)	−0.02834(35)
$\omega_e z_e$	0.001010(32)	0.001014(30)	0.00101[b]
$\omega_e a_e$	-1.5×10^{-5}	-1.5×10^{-5}	-1.5×10^{-5}
B_e	0.1897495[c]	0.1846241	0.1794985
α_e	0.001375892	0.001320652	0.001265973
	$B\,^2\Delta_{3/2u}$ state		
T_e	21913.42(104)	21913.11(104)	21913.42[b]
ω_e	284.49(36)	281.03(36)	276.67(22)
$\omega_e x_e$	1.533(41)	1.543(42)	1.425(21)
$\omega_e y_e$	−0.0094(18)	−0.00666(188)	−0.00990(52)
$\omega_e z_e$	0.000157(27)	0.000117(28)	0.000157[b]
$\omega_e a_e$	-2.0×10^{-6}	-2.0×10^{-6}	-2.0×10^{-6}
B_e	0.1617407[c]	0.1573721	0.1530031
α_e	0.001193303	0.001146015	0.001098608
H_{SO}^{AB}	240.58(67)	241.44(73)	240.58[b]
Std. Error	0.70	0.69	0.99
# Fitted transitions	60	59	46

[a]Standard deviations in parenthesis are 1σ. Constants without parentheses were fixed at preliminary values in the final analysis.
[b]Fixed at $^{35}Cl_2^+$ value.
[c]Rotational constants $[B_v = B_e - \alpha_e(v + \frac{1}{2})]$ from the *ab initio* PECs that were used in the RKR calculations to determine the vibrational overlaps.

of low order Dunham expansion fits of vibrationally resolved data. The vibrational constants up to $\omega_e z_e$ were varied but, due to correlations, the $\omega_e a_e$ constants had to be fixed in the final least squares analysis. Beyond $v' = 32$, the constants did not predict subsequent transitions, particularly those to the *B* state, very well and the least squares standard error increased rapidly.

Significant effort was made to try to include levels beyond $v' = 32$ in the effective Hamiltonian analysis, without success. Although the *ab initio* vibrational levels of the *A* and *B* state diabatic potentials were readily fitted with a limited Dunham expansion, high order Dunham constants were not least squares determinable in fitting the experimental data. We also attempted to include a vibrational level dependent spin-orbit interaction expression of the form $H_{SO} = H_{SO}^{AB} + \alpha\,[R_c - R(v_A, v_B)]$ where R_c is the bond length at the curve crossing, with interaction matrix element H_{SO}^{AB}. $R(v_A, v_B)$ is the R-centroid of any two vibrational levels, calculated from the PECs using LeRoy's Level 8.0 program.[39] This did not improve the overall standard error significantly and the standard deviation of α was comparable to its error. Attempts to include bound-free vibrational overlaps also did not lead to any improvement.

In the final analysis, transitions up to $v = 32$ were fitted for each of the chlorine isotopologues, and the results are summarized in Table V. The $^{35}Cl_2^+$ and $^{35}Cl^{37}Cl^+$ data sets were comparable and in each case ~60 transitions were fitted with an overall standard error of ~0.7 cm^{-1}. The $^{37}Cl_2^+$ data set was more sparse, particularly at low v, and we found that fewer constants could be varied, so some were fixed at their $^{35}Cl_2^+$ values, resulting in a higher overall standard error (0.99 cm^{-1}) for the 46 fitted transitions. However, in all three cases, the fitting process went very smoothly, readily predicting higher transitions, and weak or overlapped bands, up to the limit of $v' = 32$. The full details of the least squares results are presented in the supplementary material.[29]

VI. DISCUSSION

The effective Hamiltonian calculations show that the perturbations of the *A* state $\Omega = 3/2_u$ levels with $v \leq 32$ can be successfully fitted using a $\Delta\Omega = 0$ spin-orbit interaction with a constant H_{SO}^{AB} electronic interaction term. However, it is important to recognize that the matrix elements are large and thus the *A* state vibrational level shifts are substantial and involve significant interactions with several *B* state vibrational levels. For example, in the absence of the spin-orbit interaction, the *B* state $v = 0$ level occurs between the $v = 3$ and 4 levels of the *A* state and the $^{35}Cl_2^+$ coupling matrix elements $\langle A\ v_A\ |H_{SO}|\ B\ v_B = 0\rangle$ are 53 cm^{-1} for $v_A = 0$, 98 cm^{-1} for $v_A = 1$, 122 cm^{-1} for $v_A = 2$, 120 cm^{-1} for $v_A = 3$, and 97 cm^{-1} for $v_A = 4$. As a result of these interactions, as well as those with energetically more distant vibrational levels of the *B* state, the *A* state $v = 0$–4 levels are pushed down from above and the low-lying *B* state levels are pushed upwards, such that $v_A = 4$ is displaced by −133 cm^{-1} and $v_B = 0$ by +139 cm^{-1}. The level displacements get progressively smaller at higher energy so that they seldom exceed 20 cm^{-1} above $v_A = 10$.

In our least squares analysis, each observed level has one basis function with a coefficient greater than 0.5 so that assignments can still be made, and generally the second largest coefficient is for the other electronic state, in agreement with the coupled equations results. For example, bands 11 and 12 (Table I) are calculated to have the coefficients $(Av;Bv)$ $A7 = 0.54$; $B4 = 0.81$ and $A7 = 0.79$; $B4 = 0.53$, respectively. As in this example, the bands generally occur in matched pairs because of near-degeneracies, although there is also mixing with a plethora of energetically remote basis states.

Our results also explain why the rotational structure of the bands in the spectrum appears largely unperturbed. The interactions are primarily between energetically distant vibronic states, affecting each excited state rotational level of a given vibrational level in a similar manner. Simple 2×2 matrix calculations show that the rotational structure will be slightly modified but will still fit the usual $F(J) = B_v\,J(J+1) - D_v\,[J(J+1)]^2$ expression although the D_v values often exhibit anomalous negative signs, precisely as found by previous workers.[9,10] The *B* values are also modified slightly reflecting the fact that intrinsically the rotational constant in the *A* state ($R_e = 2.25$ Å) is larger than that of the *B* state ($R_e = 2.44$ Å).

It is noteworthy that the least squares determined value of $H_{SO}^{AB} = 240$ cm^{-1} is identical to the *ab initio* result obtained from both the avoided crossing (see Fig. 7) and from the matrix elements of the SO matrix, attesting to the high quality of the theoretical calculations. The determined vibrational constants of the *A* and *B* states (Table V) are also very similar to those obtained from the *ab initio* curves (see

supplementary material[29]) and are, therefore, entirely reasonable. The least squares determined electronic term values of the A and B states are 366 and 413 cm^{-1} higher than the *ab initio* values and the measured A state T_0 of 20286 $\pm$ 1 cm^{-1} is comparable to the less accurate threshold photoelectron result[16] of 20382 $\pm$ 35 cm^{-1}.

The fundamental question remains: why are we unable to accurately fit transitions to vibrational levels above $v' = 32$ in our spectrum with the two-state effective Hamiltonian model? The answer is that the high vibrational levels of the A and B states are affected by interactions with the levels of other nearby electronic states. For example, the inset in Fig. 6 shows that there is an avoided crossing between the $A\ ^2\Pi_u$ state and the $2\ ^2\Pi_u$ electronic state at 3.6 Å. This kink in the A state potential occurs at a vibrational energy of ~10 000 cm^{-1} which is equivalent to v = 30–35, near the onset of our fitting problems. Nevertheless, despite such complications, the mechanism of the perturbations for the great majority of the bands in the spectrum is now quantitatively understood in substantial detail.

It is of interest to compare the present results with the ground-breaking analysis of the emission spectrum of chlorine cation published by Huberman[7] in 1966. The first column of his system I Deslandres table (Table VI, Ref. 7) corresponds precisely to the cold bands observed in our spectra and can now be assigned upper state vibrational quantum numbers. The ground state harmonic vibrational frequency, anharmonicity, isotope effects, and B_0 value are also all in good agreement with our results. His speculation about the nature of the electronic transition ($A\ ^2\Pi_u - X\ ^2\Pi_g$) and the cause of the perturbations (homogeneous $\Delta\Omega = 0$ interactions with nearby $^2\Delta_u$ and $^2\Sigma_u^+$ electronic states) has also borne the test of time, proving to be largely correct.

Finally, it is important to note that our data only address half of the problem in that the jet-cooling only allows us to observe transitions to the A state $\Omega = 3/2$ levels. However, it is now clear that the $A\ ^2\Pi_{1/2u}$ levels must be perturbed by levels of the $C\ ^2\Sigma^+{}_{1/2u}$ state, which have an avoided crossing at 2.54 Å. The $C\ ^2\Sigma^+{}_{1/2u}$ zero point level occurs at approximately the same energy as v = 4 of the $A\ ^2\Pi_{1/2u}$ state. The spin-orbit matrix element, measured from the data in Fig. 7, is ~175 cm^{-1}, slightly smaller than $H_{SO}^{AB} = 240\ cm^{-1}$. From this information, one can expect that the first few $\Omega = 1/2$ transitions will appear to be relatively unperturbed but interloper C state levels will appear above ~v = 4, mirroring the vibrational structure and perturbations observed in the $\Omega = 3/2$ spectrum. If the transitions to the lower levels could be observed, the vibrational numbering would be clear and they could be extrapolated to the $\Omega = 1/2$ transitions reported in the literature, the data could be fitted as in the present work, and Huberman's[7] band system II would also be quantitatively understood.

VII. CONCLUSIONS

The LIF spectrum of jet-cooled chlorine cation has been recorded and the observed transitions identified as $A\ ^2\Pi_{3/2u} - X\ ^2\Pi_{3/2g}$. The 0–0 band has been positively assigned and the onset of strong homogeneous spin-orbit perturbations accompanied by the sudden appearance of interloper bands has been observed. High level *ab initio* calculations including spin-orbit coupling show an avoided crossing between the $A\ ^2\Pi_{3/2u}$ and $B\ ^2\Delta_{3/2u}$ potential curves which is the cause of the observed perturbations. Solution of the nonadiabatic coupled equations in the SO-diabatic basis provided a detailed description of the low-lying transitions, allowing definitive vibronic assignments to be made for the first time. Starting from these calculations, we were able to fit all of the observed bands in the spectrum up to $v' = 32$ to an effective Hamiltonian SO-diabatic model incorporating a single electronic spin-orbit coupling term and vibrational overlaps between the bound vibrational levels of the two states. This work provides a quantitative treatment and thorough understanding of this highly perturbed spectrum.

ACKNOWLEDGMENTS

This paper is dedicated to Fernando P. Huberman who, lacking most of the advantages of modern theory and instrumentation, still got so many aspects of the chlorine cation puzzle correct in his pioneering (1966) analysis of the emission spectrum. D.J.C. is grateful to Michael Morse and Robert Le Roy for valuable discussions about various aspects of this work. The research of the Clouthier group was supported by National Science Foundation (NSF) Grant No. CHE-1106338. R.W.F. acknowledges support from NSF Grant No. CHE-1058709.

[1] Y. Uchida and Y. Ota, Jpn. J. Phys. **5**, 53 (1928).
[2] A. Elliott and W. H. B. Cameron, Proc. R. Soc. London, Ser. A **158**, 681 (1937).
[3] A. Elliott and W. H. B. Cameron, Proc. R. Soc. London, Ser. A **164**, 531 (1938).
[4] H. G. Howell, Proc. Phys. Soc. A **66**, 759 (1953).
[5] P. B. V. Haranth and P. T. Rao, Indian J. Phys. **32**, 401 (1958).
[6] V. V. Rao and P. T. Rao, Can. J. Phys. **36**, 1557 (1958).
[7] F. P. Huberman, J. Mol. Spectrosc. **20**, 29 (1966).
[8] R. P. Tuckett and S. D. Peyerimhoff, Chem. Phys. **83**, 203 (1984).
[9] J. C. Choi and J. L. Hardwick, J. Mol. Spectrosc. **137**, 138 (1989).
[10] J. C. Choi and J. L. Hardwick, J. Mol. Spectrosc. **145**, 371 (1991).
[11] S. K. Bramble and P. A. Hamilton, J. Chem. Soc., Faraday Trans. **86**, 2009 (1990).
[12] A. W. Potts and W. C. Price, Trans. Faraday Soc. **67**, 1242 (1971).
[13] A. B. Cornford, D. C. Frost, C. A. McDowell, J. L. Ragle, and I. A. Stenhouse, J. Chem. Phys. **54**, 2651 (1971).
[14] V. H. Dibeler, J. A. Walker, K. E. McCulloh, and H. M. Rosenstock, Int. J. Mass Spectrom. Ion Process. **7**, 209 (1971).
[15] H. Van Lonkhuyzen and C. A. De Lange, Chem. Phys. **89**, 313 (1984).
[16] T. Reddish, A. A. Cafolla, and J. Comer, Chem. Phys. **120**, 149 (1988).
[17] A. Y. Yencha, A. Hopkirk, A. Hiraya, R. J. Donovan, J. G. Goode, R. R. J. Maier, G. C. King, and A. Kvaran, J. Phys. Chem. **99**, 7231 (1995).
[18] J. Li, Y. Hao, J. Yang, C. Zhou, and X. Mo, J. Chem. Phys. **127**, 104307 (2007).
[19] W. W. Harper and D. J. Clouthier, J. Chem. Phys. **106**, 9461 (1997).
[20] S. He and D. J. Clouthier, J. Chem. Phys. **124**, 084312 (2006).
[21] J. Yang and D. J. Clouthier, J. Chem. Phys. **135**, 054309 (2011).
[22] D. J. Clouthier and J. Karolczak, Rev. Sci. Instrum. **61**, 1607 (1990).
[23] M. A. A. Clyne and I. S. McDermid, J. Chem. Soc., Faraday Trans. 2 **74**, 1935 (1978).
[24] D. L. Michalopoulos, M. E. Geusic, P. R. R. Langridge-Smith, and R. E. Smalley, J. Chem. Phys. **80**, 3556 (1984).
[25] PGOPHER, a program for simulating rotational structure, C. M. Western, University of Bristol, see http://pgopher.chm.bris.ac.uk.
[26] L. Wu, X. Yang, Y. Guo, L. Zheng, Y. Liu, and Y. Chen, J. Mol. Spectrosc. **230**, 72 (2005).

[27]T. H. Dunning, Jr., K. A. Peterson, and A. K. Wilson, J. Chem. Phys. **114**, 9244 (2001).
[28]S. R. Langhoff and E. R. Davidson, Int. J. Quantum Chem. **8**, 61 (1974); E. R. Davidson and D. W. Silver, Chem. Phys. Lett. **52**, 403 (1977).
[29]See supplementary material at http://dx.doi.org/10.1063/1.4765334 for a table of the spectroscopic constants of $^{35}Cl_2^+$ obtained from the MRCI PEC's and detailed results of the least squares fitting for the three isotopologues.
[30]A. Berning, M. Schweizer, H.-J. Werner, P. J. Knowles, and P. Palmieri, Mol. Phys. **98**, 1823 (2000).
[31]L. J. Padziemski and V. Kaufman, J. Opt. Soc. Am. **59**, 424 (1969).
[32]Yu. Ralchenko, A. E. Kramida, J. Reader, and NIST ASD Team, NIST Atomic Spectra Database, version 4.1.0 (National Institute of Standards and Technology, Gaithersburg, MD, 2011), see http://physics.nist.gov/asd.
[33]H.-J. Werner, P. J. Knowles, F. R. Manby, M. Schütz *et al.*, MOLPRO, version 2010.1, a package of *ab initio* programs, 2010, see http://www.molpro.net.
[34]M. Born, Gott. Nachr. Math. Phys. Kl. **1**, 1 (1951).
[35]H. Lefebvre-Brion and R. W. Field, *The Spectra and Dynamics of Diatomic Molecules* (Elsevier, Amsterdam, 2004).
[36]L. Fox and E. T. Goodwin, Philos. Trans. R. Soc. London **245**, 501 (1953).
[37]O. Atabek and R. Lefebvre, Chem. Phys. **52**, 199 (1980).
[38]R. J. Le Roy, "RKR1 2.0: A computer program implementing the first-order RKR method for determining diatomic molecule potential energy functions," University of Waterloo Chemical Physics Research Report No. CP-657R, 2004.
[39]R. J. Le Roy, "LEVEL 8.0: A computer program for solving the radial Schrödinger equation for bound and quasibound levels," University of Waterloo Chemical Physics Research Report No. CP-663, 2007.